Available online at www.sciencedirect.com
SCIENCE DIRECT
Catalysis Today 107–108 (2005) 12–22
CATALYSIS TODAY
www.elsevier.com/locate/cattod

The role of reaction pathways and support interactions in the development of high activity hydrotreating catalysts

Henrik Topsøe [a,*], Berit Hinnemann [b], Jens K. Nørskov [b], Jeppe V. Lauritsen [c], Flemming Besenbacher [c], Poul L. Hansen [a], Glen Hytoft [a], Rasmus G. Egeberg [a], Kim G. Knudsen [a]

[a] *Haldor Topsøe A/S, Nymøllevej 55, DK-2800 Lyngby, Denmark*
[b] *Center for Atomic-scale Materials Physics, Department of Physics, Technical University of Denmark, DK-2800 Lyngby, Denmark*
[c] *Department of Physics and Astronomy, Interdisciplinary Nanoscience Center (iNANO), University of Aarhus, DK-8000 Aarhus C, Denmark*

Available online 26 August 2005

Abstract

Scanning tunneling microscopy (STM) investigations have recently provided the first atom-resolved images of reaction intermediates in the key steps of the hydrogenation (HYD) and direct desulfurization (DDS) pathways in hydrodesulfurization over MoS_2 nanoclusters. Surprisingly, special brim sites exhibiting a metallic character are observed to be involved in adsorption, hydrogenation and C–S bond cleavage. The insight is seen to provide a new framework for understanding the DDS and HYD pathways and the role of steric hindrance and poisons. Density functional theory (DFT) calculations have illustrated how support interactions may influence the activity of sulfided catalysts. The brim sites and the tendency to form vacancies are seen to differ in types I and II Co–Mo–S. High-angle annular dark-field scanning transmission electron microscopy (HAADF-STEM) studies show that the high activity Type II structures may be present as single sulfide sheets. Thus, stacking is not an essential feature of Type II catalysts. The article illustrates how the new scientific insight has aided the introduction of the new high activity BRIM^{TM} type catalysts for FCC pre-treatment and production of ultra low sulfur diesel (ULSD).

Keywords: Hydrodesulfurization; STM; DFT; HAADF-STEM; ULSD; Support interaction; Hydrogenation; Active sites; MoS_2; Nanoclusters; Thiophene; CoMo catalysts; Type II Co–Mo–S; Brim sites

1. Introduction

The legislative requirements for ultra low sulfur transport fuels have resulted in new hydrodesulfurization (HDS) challenges for the refining industry [1–9]. In addition to the issues related to the legislative drive for removing sulfur, the refiners are also faced with a growing demand for diesel fuels. This demand may partly be met by producing less low value products such as heating oil. There is also a desire to convert heavy fractions by hydrocracking or 'mild hydrocracking' processes and one may introduce upgrading processes e.g. for light cycle oil.

In order to produce low sulfur transport fuels, the refiner may choose between different revamp or grassroots options and the most cost-effective solution will depend on the specific refinery situation with respect to configuration, feedstock blends and product-slate. The selection of catalyst types is an important decision. As sulfur conversion increases, we are left with the most refractory species, typically dialkylated dibenzothiophenes [1,3,4,6,10–12]. Under idealized conditions, the conversion of these sterically hindered molecules mainly proceeds via a pre-hydrogenation route (HYD) instead of the direct desulfurization route (DDS) which is dominating for molecules like DBT [1,3,4,6,10]. Since NiMo catalysts are generally more active for the indirect hydrogenation route and CoMo catalysts more active for the direct route, one could imagine that NiMo would be the preferred option for ultra deep

* Corresponding author.
E-mail address: het@topsoe.dk (H. Topsøe).

0920-5861/$ – see front matter © 2005 Elsevier B.V. All rights reserved.
doi:10.1016/j.cattod.2005.07.165

desulfurization. However, at low hydrogen pressures and high space velocities, CoMo catalysts are often seen to outperform NiMo catalysts [5]. One of the factors, which may also influence the choice of the catalyst, is the presence of nitrogen compounds in the feed which may inhibit the reactions [1,6,8,12,13–18]. Detailed studies of inhibition effects under real feed conditions [17] have revealed that it is especially specific basic nitrogen compounds that have an effect on the HDS and HDN activity. Although the nitrogen compounds inhibit both the direct and indirect desulfurization pathways, the effect is largest for the latter. Thus, selection of catalyst depends on both feedstock and operation conditions. It is furthermore important to consider the hydrogen availability [19] and the different deactivation rates of the DDS and HYD pathways.

The details of the HDS mechanism are poorly understood, since for a long time only limited direct information has been available regarding the nature of the sites involved in the different reaction pathways [1]. This situation has recently changed and we will presently discuss STM results and the DFT calculations which have provided direct images of key sites and reaction intermediates [20–24]. Of particular importance is the observation of a new class of fully sulfur-coordinated sites, the so-called brim sites, which may play a role in the HYD pathway. We will discuss how the presence of such sites may explain different catalytic and poisoning characteristics.

Recently, DFT studies [25] have been used to provide insight into support interactions and the origin of the activity differences between Type I and Type II MoS_2 and Co–Mo–S. It is seen that support interactions may cause large changes in the tendency to form vacancies and in the properties of the brim sites. Although support interactions may also influence the tendency to form stacked MoS_2 layers, HAADF-STEM studies [26] show that the active Type II structures may be present as single-layer.

The improved scientific understanding of key factors influencing the activity and selectivity of hydrotreating catalysts has had a significant impact on catalyst design and development. The present article discusses the development of the BRIM^{TM} family of improved ULSD and FCC pre-treat catalysts.

2. Active sites and reaction pathways

The information regarding active sites and reaction pathways has in the past mainly been inferred from structure–activity correlations and kinetic studies [1,4,6]. The correlations have suggested that the active sites are located at the edges of the MoS_2 or Co–Mo–S nanoclusters. Furthermore, since the early studies of Lipsch and Schuit [27] and Kolboe [28], it has been widely accepted that the active sites are vacancies or coordinatively unsaturated sites created in a reaction with hydrogen [1]. It has been proposed that the vacancies will have an affinity for direct σ-type bond formation with the sulfur atom of the reactant. Likewise, it has also been assumed that the vacancies will also bind H_2S and that this is the origin of the H_2S inhibition effects found in many studies [1]. Although the above simple picture can explain many observations, there exists little information on the nature of vacancies and their role. Furthermore, the simple picture does not explain that molecules, like dibenzothiophene (DBT) and 4,6-dimethyldibenzothiophene (4,6-DMDBT), are desulfurized by two pathways, a direct desulfurization pathway (DDS) and a hydrogenation pathway (HYD) [3,10]. Also, it has not been understood in detail why the relative role of the two pathways varies significantly with the type of reactant molecule and the presence of poisons.

It has been observed that DBT is mainly being desulfurized by the DDS pathway, whereas 4,6-DMDBT predominantly reacts via the HYD pathway depending on feedstock and operating conditions [1–6,8,11,29]. The dramatic decrease in the DDS pathway with alkyl substitutes is generally interpreted based on the above-mentioned vacancy type mechanism. The alkyl groups located close to the sulfur atom are expected to introduce a steric hindrance and make the σ-type (η_1) interaction with the vacancy difficult.

The HYD pathway is generally assumed to proceed via π-bonding of the reactant to the catalyst surface [11]. In this flat wise adsorption mode, the alkyl substitutes are expected to give rise to less steric hindrance. Separate adsorption experiments also show that 4,6-DMDBT adsorbs with similar adsorption strength as DBT [30]. Although there appears to be general agreement on the π-type bonding, there is a large disagreement in the literature regarding the nature of the sites involved in the hydrogenation reaction [1,4,6,8,11,31]. Many authors have proposed that the sites for hydrogenation are also vacancies at the edges, but that they are different from the vacancies involved in the DDS pathway. In order to accommodate the required flat π-bonding, more open multi-vacancy sites have been advocated. For example, it was suggested [31,32] that the hydrogenation occurs on the Mo edges with exposed naked Mo atoms since such atoms could be expected to be involved in π-bonding of large reactant molecules. Several other authors have considered reactions involving naked Mo edges [33–36]. However, the DFT studies by Byskov et al. [37] showed that the exposure of naked Mo atoms is not favored. This and later studies [38–40] have calculated the most favorable structures at the Mo edges for different sulfiding and reaction conditions. The studies also show that it is not favorable to have singly bonded sulfur monomers at the edge, since they tend to reconstruct into dimers with significant sulfur–sulfur binding. Other edge reconstructions may also be encountered, but, as mentioned above, it was found very unfavorable energetically to create multiple vacancies in the different structures. In light of these new results there is a need for re-addressing our thinking regarding the nature of the HYD pathway and the sites

involved in such reactions. It is important that a new model can explain the different observations including the fact that the HYD pathway is not severely poisoned by H_2S, an observation which is not easily explained by a mechanism involving highly coordinatively unsaturated Mo edge sites. The recent introduction of STM measurements as a surface science tool in hydrotreating catalysis research has allowed important progress to be made since we can now obtain atom-resolved images of the active MoS_2-like nanoclusters and thereby directly monitor the morphology, reveal the atomic-scale structure, pinpoint adsorption sites and resolve signatures of reaction intermediates [20–24]. Below we will discuss some of these results obtained on relevant hydrodesulfurization model catalysts consisting of sulfide nanoclusters grown on an inert gold substrate.

Fig. 1 shows an atom-resolved STM image of a MoS_2 nanocluster. The MoS_2 cluster has a size of ∼3 nm and consists of a single MoS_2 layer (one S–Mo–S sheet). Interestingly, under the experimental conditions, the preferred shape of the clusters was observed to be triangular. Therefore, the clusters only expose one of the two types of low-index MoS_2 edges. A detailed analysis involving theoretical DFT calculations shows that the exposed edges are the Mo edges. In view of the previous discussion it is interesting to stress that the analysis shows that the edges do not expose the ''naked'' Mo atoms which have previously been proposed to account for the hydrogenation reactions. In fact a detailed analysis of the atomic details of the MoS_2 nanoclusters in the STM images shows in agreement with DFT calculations that the clusters are fully saturated with sulfur, which forms dimers.

The atom-resolved STM images furthermore reveal a pronounced bright brim located on top of the triangular MoS_2 nanocluster adjacent to the edge itself. This brim extends all the way around the MoS_2 cluster. It should be mentioned that an STM image recorded in the so-called constant-current mode can be regarded as contours of constant local density of electronic states (LDOS) at the Fermi level. Thus the bright brim observed with STM (Fig. 1) reflects regions of high electron density. Electrons are found to be confined perpendicular to the cluster edges in a narrow region, and the brim arises from a perturbation of the electronic structure of MoS_2 near the edges. By analysis of the electronic band structure it is found that so-called one-dimensional edge states exist. These cross the Fermi level and thereby render the edges metallic as opposed to the semiconductor interior of the cluster. This unexpected electronic feature is a result of the way in which the MoS_2 nanocrystal is terminated and the properties of the brim states are, as we shall discuss later, sensitive to changes occurring at the edge including bonding to the support. Detailed DFT calculations [23,40,41] show that the brim states originate from d–d bonds between the first row of Mo atoms and p–d bonds between the second row of sulfur atoms and the Mo atoms behind. When the different electronic features calculated by DFT are taken into account, one may simulate very well the observed STM images. Although many of the observed features are quite different from the views of MoS_2 which were presented previously, they can, however, all be understood in detail. For the present discussion of the catalytic properties it is important to emphasize that the region at the brim is fully saturated by sulfur, and that we do not observe the brim states to result from the presence of vacancies.

The STM results [22,24] reveal that the unusual electronic states associated with the brim may facilitate the formation of stable bonds to thiophene. The experiment was performed by exposing the fully sulfided clusters to thiophene from the gas phase; and by imaging the clusters afterwards with STM in atomic detail, it was possible to image directly the location of adsorbed species and the nature of reaction intermediates. Fig. 2 shows an image of a MoS_2 cluster after exposure to thiophene at low temperature ($T < 200$ K). The main observation is that the thiophene clearly prefers to adsorb onto sites directly on top of the brim (Type B in the figure). Fig. 2 shows that thiophene adsorbs in chain-like structures along the brim. The appearance and dimension of the thiophene in the STM images suggest that

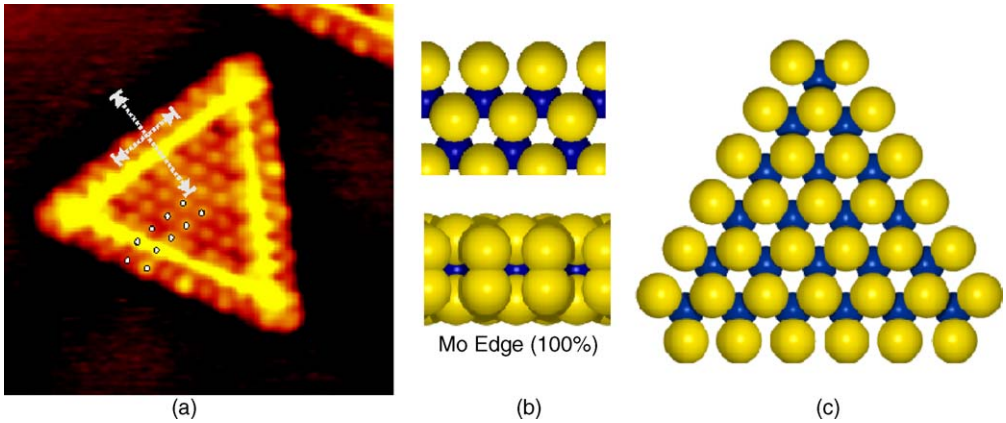

Fig. 1. (a) Atom-resolved STM image of a triangular single-layer MoS_2 nanocluster (67 × 69 Å^2). (b) Ball models in top and side view of the edge structure, the Mo edge with S dimers (S, bright; Mo, dark). (c) Ball model of a MoS_2 triangle exposing this type of edge termination [24].

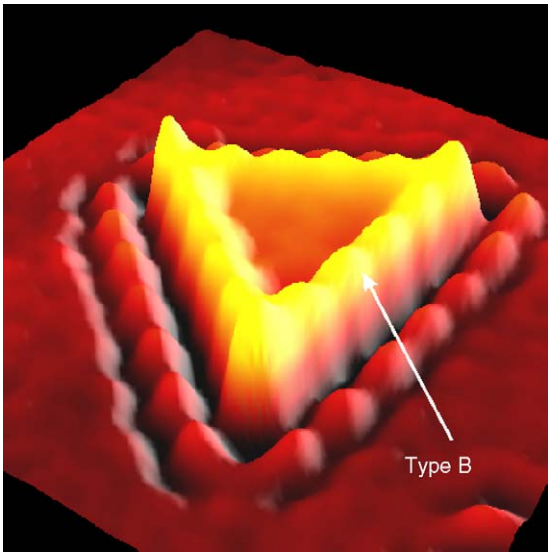

Fig. 2. STM image showing the adsorption of thiophene on triangular MoS_2 clusters at low temperature. Type B represents thiophene molecules adsorbed in positions on top of the brim states [24].

the thiophene is π-bonded to the brim state in a flat η^5 like adsorption geometry. This adsorption geometry may account for previous spectroscopic (vibration) results [42–44]. Further experiments show that the thiophene is not very strongly bound, but the brim sites are clearly able to facilitate the formation of stable bonds to thiophene. From a catalytic point of view, the type of bonding properties associated with the brim is very interesting, since a good catalyst is often characterized by a bonding of intermediate strength. In contrast, the interior basal plane sites do not bind thiophene even at the low temperature of this experiment, supporting the general view that such sites are chemically inert and do not play a role in the catalysis [1]. The STM results have therefore provided information on possible initial adsorption geometries which under reaction condition may lead to hydrodesulfurization reactions. Such reactions do not take place in this experiment, since the MoS_2 cluster imaged (Fig. 2) does not contain hydrogen and upon heating the adsorbed thiophene simply desorbs without undergoing further reactions.

In order to understand hydrotreating reactions it is important also to gain insight into the reactions related to the activation of hydrogen on the MoS_2 nanoclusters and the likely location of the adsorbed hydrogen species. Previous results show that SH groups may form [45–47] and one study indicated that these groups are located at the MoS_2 edges [45]. The STM and DFT studies [24,40,48] provided more detailed insight into the activation and location of hydrogen in these structures. The experiments show that the activation of molecular hydrogen is inhibited due to the low pressures of hydrogen. This is related to a rather high activation barrier for the dissociation of hydrogen under the conditions of the experiment, but by dosing pre-dissociated hydrogen this barrier can be removed and hydrogen can be adsorbed. The STM experiments show that adsorption of hydrogen on the MoS_2 nanoclusters (Fig. 3) preferentially occurs on the sulfur dimers and leads to the formation of SH groups on the edge. Theoretical calculations show that the most stable position of hydrogen is on top of the S atom adjacent to the brim states (Fig. 3). The combination of hydrogen adsorbing on the edge and the unusual brim sites capable of adsorbing thiophene may be an important feature in terms of hydrogenation, since the close vicinity of the reactants may promote the reaction. Before discussing such a mechanism further, it is noted that exposure to pre-dissociated hydrogen also leads to vacancy formation on the edges [20,24]. STM images reveal that typically one or two vacancies may form on the edge. Thus the SH groups may play an essential role, both in the creation of vacancies and in providing hydrogen for the hydrogenation reactions.

When thiophene is exposed to the MoS_2 nanoclusters containing SH groups, STM images now show that reactions readily occur and by imaging the clusters in atomic detail it is possible to find signatures of reaction intermediates

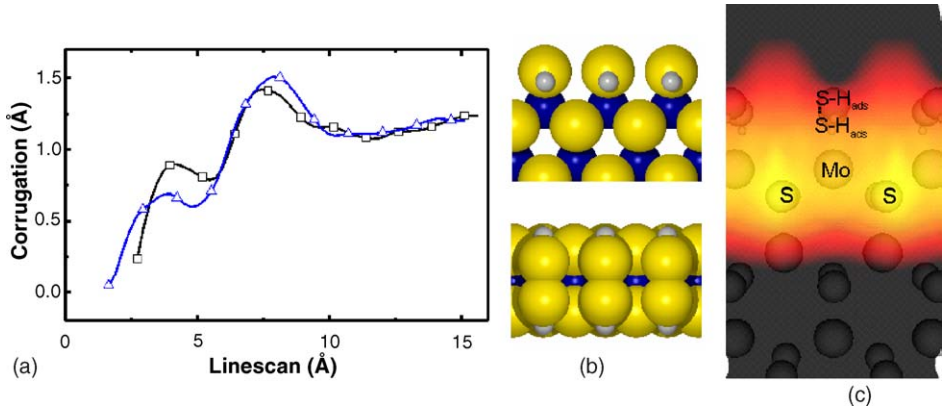

Fig. 3. (a) Representative STM line scans drawn perpendicular to the fully sulfided Mo edge of the MoS_2 nanoclusters prior to (squares) and after (triangles) exposure to pre-dissociated hydrogen. (b) Ball models of the proposed structures with adsorbed hydrogen as SH groups. (c) STM simulation showing quantitative and qualitative agreement with the experiment [24,40].

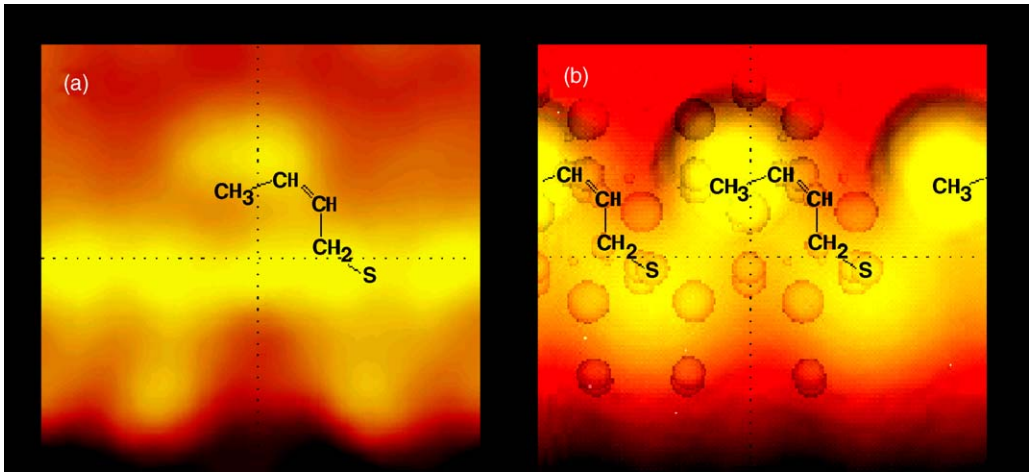

Fig. 4. (a) Close-up of an STM image showing the MoS_2 edge region with a single *cis*-but-ene-thiolate (C_4H_7S) molecule adsorbed on the metallic brim states. (b) DFT-based STM simulation of the same part of the MoS_2 edge region. Atomic balls imbedded in the STM simulation indicate the positions of Mo (large) and S (small) atoms. The molecular skeleton model shows the most stable thiolate structure found from the DFT calculations [24].

adsorbed on the clusters [24]. In the STM image (Fig. 4), it is observed that bean-like structures are located near the brim extending from the brim and inwards. Typically every MoS_2 nanocluster contains several such structures all adsorbed in the same configuration spanning the brim. Since the features only occur after exposure to hydrogen, the STM results strongly suggest that the observed species are reaction intermediates resulting from a hydrogenation reaction, involving a reaction of the SH groups with thiophene initially adsorbed on the brim sites.

The identity of the molecular species was established by calculating the stable structure for many different possible intermediates and comparing the resulting simulated STM images with the experimental STM images (Fig. 4). The best match was found for *cis*-but-2-ene-thiolate. Surprisingly, the adsorption on the brim sites has not only facilitated a hydrogenation reaction, but bond cleavage of the first C–S bond in the thiophene has also occurred. In the calculation the sulfur of the thiolate is seen to be adsorbed on top of one of the sulfur atoms of the brim indicating a direct interaction with a fully sulfided part of the cluster. The hydrocarbon end of the thiolate is located inside the brim and is therefore less involved in the bonding.

The thiolate corresponds simply to an adsorbed butenethiol, which is expected to be much more reactive than the aromatic-like thiophene [1] and the fact that we are able to observe the intermediate is probably related to the experimental conditions. Some thiolates may have reacted with SH groups and the resulting thiol will have desorbed/reacted and will consequently not be imaged. The remaining thiolates are very mobile, but they do not react further since this will require a vacancy site for accepting the sulfur atom, and under the experimental conditions such vacancies will be quenched. It is likely that no further SH groups are left on the cluster so that the remaining thiols cannot desorb but only diffuse on the cluster, and therefore it is possible to image them. Under hydrotreating reaction conditions, there will be a large population of vacancies on the edges, which may facilitate the second C–S bond cleavage, either via surface diffusion of the thiolate or via desorption of the thiol from the brim and re-adsorption and reaction on the vacancies.

When a significant vacancy concentration is available, the direct interaction of thiophene with a vacancy is also likely, and such a situation may also be imaged with STM (Fig. 5). It is well known that thiophenes may react through both the HYD and DDS pathways, and the STM image may show the initial step in the DDS pathway. DFT calculations [37] indicate that the DDS pathway may be even more favored on the S-terminated edges where vacancies are more

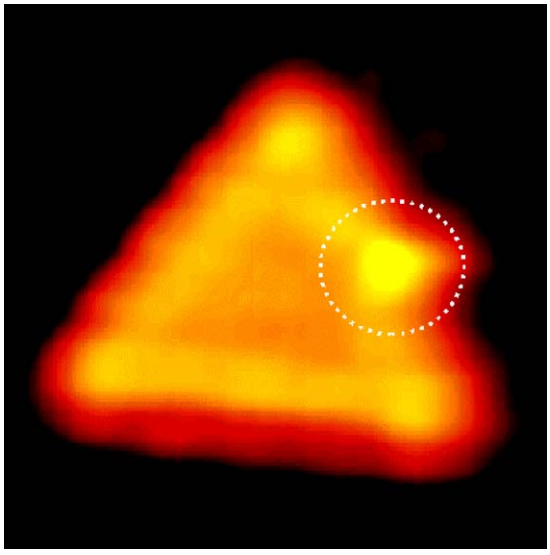

Fig. 5. STM image of a triangular MoS_2 nanocluster exposed first to atomic hydrogen, then thiophene, and finally quenched to the imaging temperature of 250 K. The large protrusion at the edge (indicated by a circle) possibly identifies either an intact thiophene molecule coordinated end-on to a vacancy or a hydrogenated derivative coordinated through the terminal S atom [24].

easily formed. The STM results also show that the vacancies are easily quenched in agreement with the strong inhibition by H_2S of the direct desulfurization pathway. The insight into the direct desulfurization pathway is very much in line with the picture researchers have assumed for this pathway. However, it is interesting that by quenching the direct pathway, the STM experiments have also allowed insight into the HYD pathway. The emerging picture is very different from previous models for this pathway. Nevertheless, the mechanism involving the brim sites allows many observations to be explained which were difficult to rationalize in previous models. A few examples are given below. The lack of strong inhibition by H_2S was difficult to understand in previous models which involved highly coordinatively unsaturated sites. This is now readily understood since the brim sites are fully coordinated by sulfur and do not adsorb H_2S. The STM results indicate that the last reaction step of the HYD pathway may take place on the same type of vacancy sites as those involved in the DDS pathway. In agreement with this, detailed kinetic experiments [49] have recently shown that the final sulfur removal step in the HYD pathway of 4,6-DMDBT was inhibited by H_2S to the same extent as the DDS pathway. The observed flat π-bonding mode of thiophene on the brim sites is also consistent with the hydrogenation pathway being less sensitive to alkyl substitutes in the reactants [1–6,8,11,24]. The tendency of other compounds present in the oil to form π-bonds may explain the origin of their inhibition effects. The large inhibition effects of basic nitrogen compounds [1,6,8,12–17,50] may be related to possibilities that such molecules may gain extra stability by also interacting with the neighboring acidic SH groups. Presently we are investigating such effects further.

3. Support interactions and the origin of Type I/II Co–Mo–S structures

The role of support interactions in HDS catalysts has been a central topic in many scientific investigations [1,51]. Also from an industrial point of view, this is a very important topic since changing support properties are some of the key parameters used to control catalyst activity and selectivity. Most studies have dealt with the industrially important alumina-supported NiMo or CoMo catalysts. One of the main advantages of using alumina as a support is the easy formation of small stable MoS_2 nanoclusters. These will have a high MoS_2 edge dispersion which is important since it increases the amount of Co (Ni) that can be accommodated in the form of the active Co–Mo–S (Ni–Mo–S) structures [1]. Besides this stabilizing effect, the support interaction may also influence the intrinsic activity of the active sites in the Co–Mo–S structures. For example, several years ago we observed [52] that increasing the sulfiding temperature may result in modified Co–Mo–S structures with substantially higher activity per Co edge atom than those formed at the lower temperature. The high and low activity forms of Co–Mo–S were termed types II and I Co–Mo–S, respectively. The Type I Co–Mo–S structures were proposed to be incompletely sulfided and have some remaining Mo–O–Al linkages to the support [52]. The presence of such linkages was related to the interaction which occurs in the calcined state between Mo and surface alumina OH groups leading to oxygen bridged monolayer type structures that are difficult to sulfide completely. Several subsequent studies [53–55] have provided evidence for the existence of Mo–O–Al linkages in Type I structures. In accordance with this picture, a weak support interaction favors the creation of Type II structures. The linkages to the support may, as discussed above, be broken by high temperature sulfiding but this may not be a desirable way of producing the highly active Type II structures, since the high temperatures may result in sintering and loss of important edge sites. It is therefore desirable to find alternate production procedures, and it has been observed that the interaction with the support may be avoided by introduction of additives or chelating agents or by using weakly interacting supports such as carbon [53,56–59].

The degree of stacking of MoS_2 was observed to have an influence on the activity/selectivity of unsupported catalysts [60]. The presence of multi-stack MoS_2 structures has also been observed in catalysts containing Type II structures. However, multi-stacking may not be a necessary feature of Type II structures but just a ‘‘by-product’’ of the presence of weak support interactions. Also, there may be a tendency for stacking to accompany the breaking of support linkages. Several results have in fact indicated that it is possible to produce catalysts with single slab Type II Co–Mo–S structures [1]. The conclusions regarding MoS_2 stacking have typically been obtained by using high-resolution electron microscopy (HRTEM) [61–66]. The application of HRTEM has provided useful insight, but there are several complications, for example, not all MoS_2 structures are typically being imaged [61,66]. Furthermore, information regarding the shape and morphology of the sulfide nanoclusters is usually not obtained. Recently, we showed that such information may be obtained by use of high-angle annular dark-field scanning transmission electron microscopy (HAADF-STEM) imaging [26]. WS_2 was supported on graphite, since this support interacts weakly with the sulfide structures and easily permits the formation of Type II structures. The HAADF-STEM imaging readily allows morphology of the clusters to be obtained (Fig. 6). The intensity analysis in such experiments is quite straightforward, and it was observed that single-layer WS_2 sheets dominate. This was also observed in edge-on images (Fig. 7). In view of the role of brim sites discussed in the last section, such single slab structures will have the advantage of making more brim sites available for reaction. For multi-stack structures, only the top layer will expose the brim sites.

DFT studies [25] recently elucidated the origin of the intrinsic activity differences between types I and II

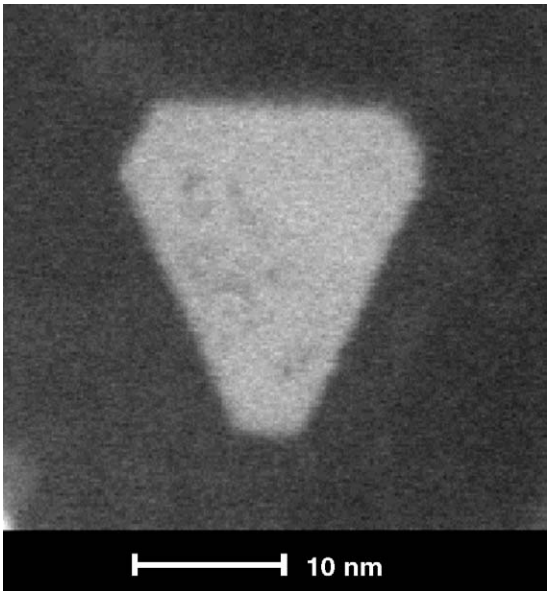

Fig. 6. HAADF-STEM image of a single-layer truncated triangular graphite supported WS_2 nanocrystal [26].

structures. The effect of the presence of linkages to the alumina on the direct desulfurization and hydrogenation pathways was addressed by calculating the difference in the Mo–S bond strength and the properties of the brim sites. The calculations also provided information on how the clusters are bonded to the alumina. It was shown that the Mo–O linkages are favored at the S edges. This is interesting since the DFT [37] and STM [21] results have shown that the Co atoms in Co–Mo–S also prefer to be located at the S edges of MoS_2. These DFT results allow one to understand why the Type I–II transition occurs at the temperature where edge saturation by Co has been reached (Fig. 8). The presence of oxygen linkages at the sulfur edge is seen to increase the energy required to form sulfur vacancies significantly (Fig. 9). Since sulfur vacancies are necessary for the DDS pathway and the final step in the HYD pathway, this is a key factor contributing to the low activity of Type I structures.

The DFT calculations [25] also addressed the influence of support linkages on the brim states. In the previous section, it was shown that having hydrogen on the edge sulfurs only had a minor influence on the brim states. However, having oxygen linkages to the support dramatically influences the brim states and reduces their metallic character (Fig. 10). While there are still metallic edge states present, the linkages lead to a significantly lower electron density at the brim and therefore to a significantly weaker brim structure in the simulated STM picture. This is expected to have a negative effect on the ability to bind reactants and catalyze reactions via the HYD pathway (see last section). Furthermore, the formation of SH groups was found to be significantly affected [25], which in turn will influence certain inhibition effects. All the above results clearly illustrate that support interactions may affect many properties influencing the different reaction pathways of HDS and other hydrotreating reactions and the overall activity/selectivity. Clearly, additives binding to the edge regions of unpromoted and promoted sulfide nanostructures are also expected to influence such properties, and a control of these effects will be critical for generating catalysts with desired properties.

4. Recent catalyst developments

In the development of new hydrotreating catalysts and technologies, we have benefited from new fundamental insight gained into all aspects of hydrotreating catalysis, ranging from studies of the active nanostructures to an understanding the complex deactivation behaviors and trickle bed flow patterns. It is clear that the new insight regarding pathways and support interaction discussed presently has many consequences for optimal catalyst

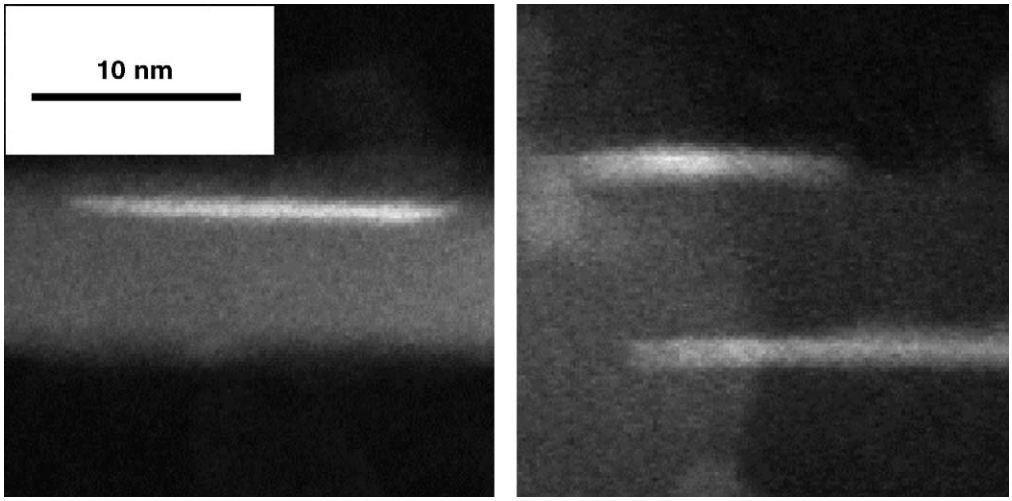

Fig. 7. HAADF-STEM image of graphite supported WS_2 nanocrystals. The graphite sheet is imaged edge on and the WS_2 crystals are single-layer [26].

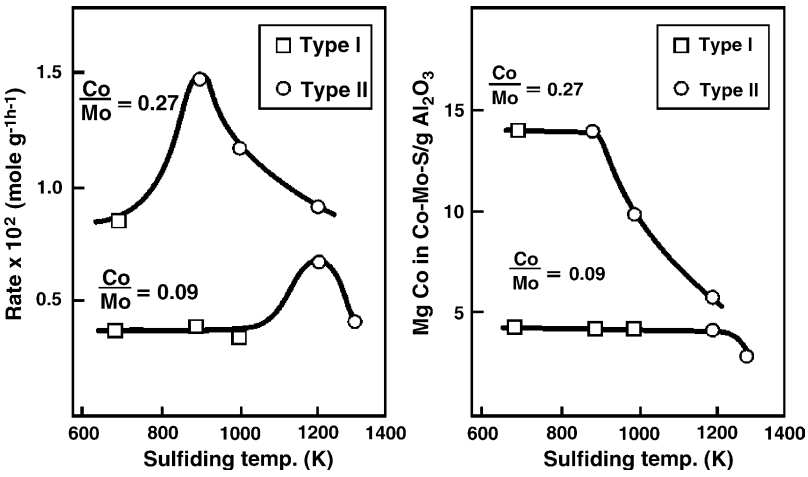

Fig. 8. The Type I–II transition behavior for two Co–Mo/Al_2O_3 catalysts [52,53].

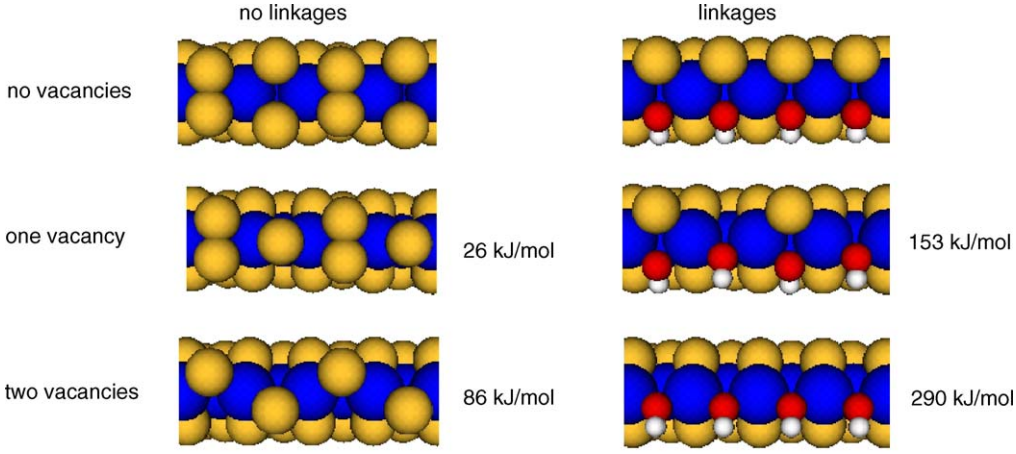

Fig. 9. The structures and energies for vacancy formation with and without linkages. All structures are calculated energy minima. The energy values denote the energy required for vacancy formation starting from the fully sulfided structures in the first line [25].

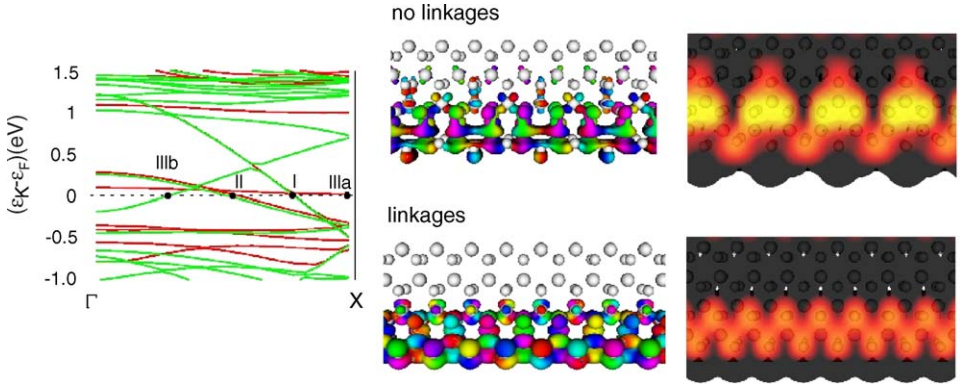

Fig. 10. The one-dimensional band structure, the contours of the Kohn-Sham wave functions and simulated STM images for the MoS_2 sulfur edge without and with oxygen linkages. In the band structure diagram, the red bands belong to the structure without linkages, and the green bands to the structure with linkages. The S edge for the structure without linkages is terminated by sulfur dimers. For the structure with oxygen linkages, they are present in every row. For both systems, edge states I and II are located at the molybdenum edge and therefore not interesting in the present context. The structure without linkages has edge state IIIa located at the sulfur edge, and the structure with linkages edge state IIIb. For the simulated STM pictures, a contour value for the local density of states of 8.3e-6 $(eV\,Å^3)^{-1}$ has been used, which has been determined to be suitable in a previous study [40]. The corrugation for both images is 1.5 Å. It should be noted that both images have been prepared with exactly the same parameters and are therefore fully comparable. [25].

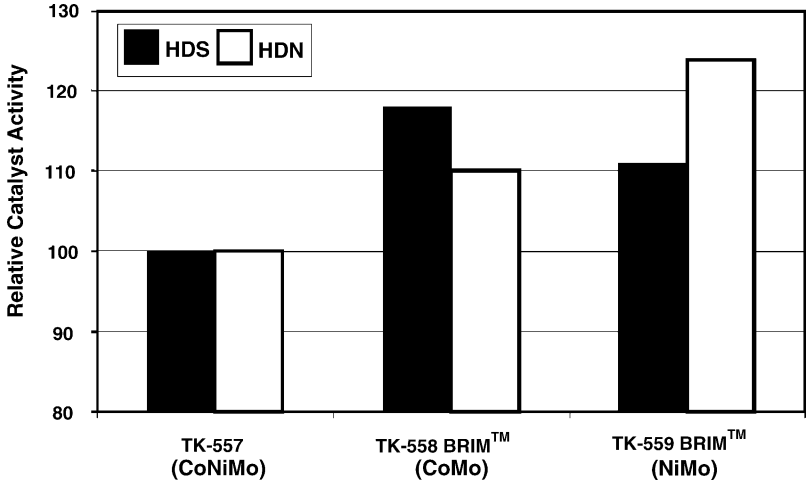

Fig. 11. Relative activities of Haldor Topsøe's BRIM™ technology catalysts for FCC pre-treatment service as observed in pilot plant tests. Both TK-558 BRIM™ and TK-559 BRIM™ show HDN and HDS activities superior to their well-recognized predecessor TK-557.

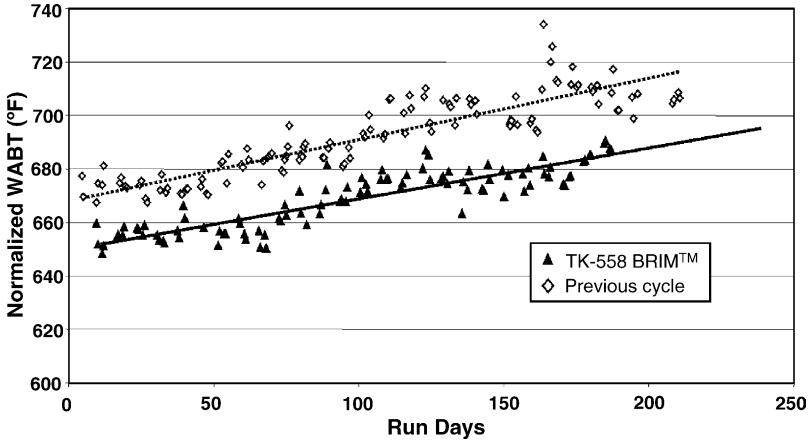

Fig. 12. Industrial performance of TK-558 BRIM™ in FCC pre-treatment operation. The normalized weighted average bed temperature (WABT) is the relative temperature needed to give the same catalytic activity as observed at the start-of-run conditions. TK-558 BRIM™ has higher activity and slightly lower deactivation rate than the catalyst used in the previous cycle.

formulations. Thus, in parallel with these findings, Haldor Topsoe has developed new supports and new preparation procedures that have resulted in a new family of high activity hydroprocessing catalysts. This new BRIM™ technology not only optimizes the brim site HYD functionality, but also increases the rate of the DDS pathway. The first two commercial catalysts based on this technology were the TK-558 BRIM™ (CoMo) and TK-559 BRIM™ (NiMo) catalysts for FCC pre-treatments service. They show superior activity (Fig. 11), excellent stability (Fig. 12), and have been successfully adopted by many refiners.

Recently, the BRIM™ technology has also resulted in a new CoMo catalyst, TK-576 BRIM™, for the production of ultra low sulfur diesel (ULSD). The advantage of this catalyst is illustrated in Table 1. It is clear that TK-576 BRIM™ is better than its predecessor, TK-574, which is among the best catalysts on the market. The feedstock for this test is a mixture of 25% light cycle oil (LCO) and 75% straight run gas oil (SRGO) diesel, and the feedstock sulfur content is above 1.8 wt.%. The difference in activity between TK-576 BRIM™ and TK-574 corresponds in many cases to around 6–12 months longer cycle length. Fig. 13 shows the stability of the new catalyst. The relative activity is shown as a function of run hours from a pilot plant test with different feedstock. The tests are carried out at a low hydrogen partial pressure and very high conversions.

Table 1
Comparison of the performance of TK-574 and -576 BRIM™ for the production of 50 and 10 ppm S diesel

	TK-574		TK-576 BRIM™	
Product sulfur, (wt) ppm	50	10	50	10
H_2 pressure, (bar)	30	30	30	30
LHSV, (hr^{-1})	1.5	1.5	1.5	1.5
WABT, (°C)	350	369	345	362

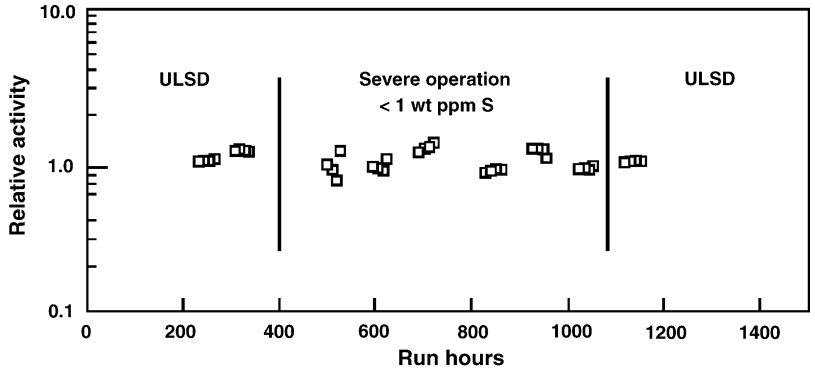

Fig. 13. TK-576 BRIM^{TM} stability test at 20 bar hydrogen partial pressure. After producing a diesel product with less than 10 wtppm sulfur (ULSD condition) from a Kuwait SRGO with 1.2 wt.% sulfur the feedstock was changed to a North Sea SRGO with 0.2 wt.% sulfur. Furthermore, the conditions were set to produce a diesel product with less than 1 wtppm sulfur. Finally, the catalyst was again tested with the Kuwait SRGO at the ULSD condition. The HDS activity is almost constant during the entire test.

5. Conclusions

The challenges that the refining industry is facing now call for major developments within hydroprocessing catalyst technology. To assess how a specific refinery successfully adjusts to the new legislation and market demands, a detailed knowledge of reaction kinetics and catalyst reactivity and selectivity is required. The progress in fundamental understanding of support interactions, catalyst morphology and direct desulfurization and hydrogenation reaction pathways has helped introduce new families of high activity catalysts for different services. Further progress in such studies is expected to continue to provide new opportunities for the development of improved commercial catalysts.

Acknowledgements

The authors would like to thank Bjerne S. Clausen, Lars Skyum, Per Zeuten, Nan-Yu Topsøe, Poul Georg Moses, Ashildur Logadottir, Anna Carlsson and Michael Brorson for fruitful discussions.

References

[1] H. Topsøe, B.S. Clausen, F.E. Massoth, in: J.R. Anderson, M. Boudart (Eds.), Hydrotreating Catalysis—Science and Technology, vol. 11, Springer Verlag, Berlin, 1996.
[2] M.V. Landau, Catal. Today 36 (1997) 393.
[3] B.C. Gates, H. Topsøe, Polyhedron 16 (1997) 3213.
[4] D.D. Whitehurst, T. Isoda, I. Mochida, Adv. Catal. 42 (1998) 345.
[5] K.G. Knudsen, B.C. Cooper, H. Topsøe, Appl. Catal. A 189 (1999) 205.
[6] T. Kabe, A. Ishihara, W. Qian, Hydrodesulfurization and Hydrogenation, Chemistry and Engineering, Wiley-CH, Kodanska, 1999.
[7] S.F. Venner, Hydrocarb. Process. 79 (2000) 51.
[8] C. Song, Catal. Today 86 (2003) 211.
[9] I.V. Babich, J.A. Moulijn, Fuel 82 (2003) 607.
[10] M. Houalla, N.K. Nag, A.V. Sapre, D.H. Broderick, B.C. Gates, AIChE J. 24 (1978) 1015.
[11] X.-L. Ma, K. Sakaanishi, I. Mochida, Ind. Eng. Chem. Res. 35 (1996) 2487.
[12] M. Breysse, G. Djega-Mariadassou, S. Pessayre, C. Geantet, M. Vrinat, G. Perot, M. Lemaire, Catal. Today 84 (2003) 129.
[13] M. Nagai, T. Kabe, J. Catal. 81 (1983) 440.
[14] M. Nagai, T. Sato, A. Aiba, J. Catal. 97 (1986) 52.
[15] V. LaVopa, C.N. Satterfield, J. Catal. 110 (1988) 375.
[16] F. van Looij, P. van der Laan, W.H.J. Stork, D.J. DiCamillo, J. Swain, Appl. Catal. A 170 (1998) 1.
[17] P. Zeuthen, K.G. Knudsen, D.D. Whistehurst, Catal. Today 65 (2001) 307.
[18] P. Wiwel, K. Knudsen, P. Zeuten, D. Whitehurst, Ind. Eng. Chem. Res. 39 (2000) 533.
[19] T. Tippet, K.G. Knudsen, B. Cooper, in: Proceedings of the NPRA Annual Meeting, Paper AM-99-06, 1999.
[20] S. Helveg, J.V. Lauritsen, E. Lægsgaard, I. Stensgaard, J.K. Nørskov, B.S. Clausen, H. Topsøe, F. Besenbacher, Phys. Rev. Lett. 84 (2000) 951.
[21] J.V. Lauritsen, S. Helveg, E. Lægsgaard, I. Stensgaard, B.S. Clausen, H. Topsøe, F. Besenbacher, J. Catal. 197 (2001) 1.
[22] J.V. Lauritsen, M. Nyberg, R.T. Vang, M.V. Bollinger, B.S. Clausen, H. Topsøe, K.W. Jacobsen, E. Lægsgaard, J.K. Nørskov, F. Besenbacher, Nanotechnology 14 (2003) 385.
[23] J.V. Lauritsen, M.V. Bollinger, E. Lægsgaard, K.W. Jacobsen, J.K. Nørskov, B.S. Clausen, H. Topsøe, F. Besenbacher, J. Catal. 221 (2004) 510.
[24] J.V. Lauritsen, M. Nyberg, J.K. Nørskov, B.S. Clausen, H. Topsøe, E. Lægsgaard, F. Besenbacher, J. Catal. 224 (2004) 94.
[25] B. Hinnemann, J.K. Nørskov, H. Topsøe, J. Phys. Chem. B 109 (2005) 2245.
[26] A. Carlsson, M. Brorson, H. Topsøe, J. Catal. 227 (2004) 530.
[27] J.M.J. Lipsch, G.C.A. Schuit, J. Catal. 15 (1969) 174.
[28] S. Kolboe, Can. J. Chem. 47 (1969) 352.
[29] F. Bataille, J.L. Lemberton, P. Michaud, G. Perot, M. Vrinat, M. Lemaire, E. Schulz, M. Breysse, S. Kasztelan, J. Catal. 191 (2000) 417.
[30] V. Meille, E. Schulz, M. Lemaire, M. Vrinat, J. Catal. 170 (1997) 29.
[31] X.L. Ma, H.H. Schobert, ACS. Div. Petrol. Chem. Prep. 213 (1997) 15.
[32] X. Ma, H.H. Schobert, J. Mol. Catal. A 160 (2000) 409.
[33] S. Kasztelan, L. Jalowiecki, A. Wambeke, J. Grimblot, J.P. Bonnelle, Bull. Soc. Chim. Belg. 96 (1987) 1003.
[34] P. Raybaud, J. Hafner, G. Kresse, H. Toulhoat, in: D. Delmon, et al. (Eds.), Hydrotreatment and Hydrocracking of Oil Fractions, Elsevier, 1999, p. 309.
[35] H. Yang, C. Fairbridge, Z. Ring, Energ. Fuels 17 (2003) 387.
[36] S. Cristol, J.F. Paul, E. Payen, D. Bougeard, F. Hutschka, S. Clemendot, J. Catal. 224 (2004) 138.

[37] L.S. Byskov, J.K. Nørskov, B.S. Clausen, H. Topsøe, J. Catal. 187 (1999) 109.
[38] P. Raybaud, J. Hafner, G. Kresse, S. Kasztelan, H. Toulhoat, J. Catal. 189 (2000) 129.
[39] S. Cristol, J.F. Paul, E. Payen, D. Bougeard, S. Clemendot, F. Hutschka, J. Phys. Chem. B 104 (2000) 11220.
[40] M.V. Bollinger, K.W. Jacobsen, J.K. Nørskov, Phys. Rev. B 67 (2003) 085410.
[41] M.V. Bollinger, J.V. Lauritsen, K.W. Jacobsen, J.K. Nørskov, S. Helveg, F. Besenbacher, Phys. Rev. Lett. 87 (2001) 196803.
[42] P.C.H. Mitchell, D.A. Green, E. Payen, J. Tomkinson, S.F. Parker, Phys. Chem. Chem. Phys. 1 (1999) 3357.
[43] P. Mills, S. Korlann, M.E. Bussell, M.A. Reynolds, M.V. Ovchinnikov, R.J. Angelici, C. Stinner, T. Weber, R. Prins, J. Phys. Chem. A 105 (2001) 4418.
[44] T.L. Tarbuck, K.R. McCrea, J.W. Logan, J.L. Heiser, M.E. Bussell, J. Phys. Chem. B 102 (1998) 7845.
[45] N.-Y. Topsøe, H. Topsøe, J. Catal. 139 (1993) 641.
[46] E. Payen, S. Kasztelan, J. Grimblot, J. Mol. Struct. 174 (1998) 71.
[47] P. Sundberg, R. Moyes, J. Tomkinson, Bull. Soc. Chim. Belg. 100 (1991) 967.
[48] L.S. Byskov, M. Bollinger, J.K. Nørskov, B.S. Clausen, H. Topsøe, J. Mol. Catal. A 163 (2000) 117.
[49] M. Egorova, R. Prins, J. Catal. 225 (2004) 417.
[50] T.C. Ho, D. Nguyen, J. Catal. 222 (2004) 450.
[51] M. Breysse, P. Afanasiev, C. Geantet, M. Vrinat, Catal. Today 86 (2003) 5.
[52] R. Candia, B.S. Clausen, H. Topsøe, in: Proceedings of the 9th Iberoamerican Symposium on Catalysis, Lisbon Portugal, 1984, p. 211.
[53] H. Topsøe, R. Candia, N.-Y. Topsøe, B.S. Clausen, Bull. Soc. Chim. Belg. 93 (1984) 783.
[54] E. Diemann, Th. Weber, A. Müller, J. Catal. 148 (1994) 288.
[55] R.G. Leliveld, A.J. van Dillen, J.W. Geus, D.C. Konigsberger, J. Catal. 165 (1997) 184.
[56] J.A.R. van Veen, E. Gerkema, A.M. van der Kraan, A. Knoester, J. Chem. Soc. Chem. Commun. 22 (1987) 1684.
[57] J.P.R. Vissers, B. Scheffer, J.H.J. de Beer, J.A. Moulijn, R. Prins, J. Catal. 105 (1987) 277.
[58] L. Medici, R. Prins, J. Catal. 163 (1996) 38.
[59] L. Coulier, G. Kishan, J.A.R. van Veen, J.W. Niemantsverdriet, J. Phys. Chem. B 106 (2002) 5897.
[60] M. Daage, R.R. Chianelli, J. Catal. 149 (1994) 414.
[61] R. Candia, O. Sørensen, J. Villadsen, N.-Y. Topsøe, B.S. Clausen, H. Topsøe, Bull. Soc. Chim. Belg. 93 (1984) 763.
[62] T.F. Hayden, J.A. Dumesic, J. Catal. 103 (1987) 366.
[63] J. Ramirez, S. Fuentes, G. Diaz, M. Vrinat, M. Breysse, M. Lacroix, Appl. Catal. 52 (1989) 211.
[64] S. Srinivasan, A.K. Datye, C.H.F. Peden, J. Catal. 137 (1992) 513.
[65] S. Eijsbouts, J.J.L. Heinerman, H.J.W. Elzerman, Appl. Catal. A 105 (1993) 53.
[66] R.M. Stockmann, H.W. Zandbergen, A.D. van Langeveld, J.A. Moulijn, J. Mol. Catal. A 102 (1995) 147.